NATIONAL ADVISORY COMMITTEE FOR AERONAUTICS

TECHNICAL NOTE

No. 1732

CALCULATED EFFECTS OF GEOMETRIC DIHEDRAL ON THE LOW-SPEED ROLLING DERIVATIVES OF SWEPT WINGS

By M. J. Queijo and Byron M. Jaquet

Langley Aeronautical Laboratory
Langley Field, Va.

Washington
October 1948

NATIONAL ADVISORY COMMITTEE FOR AERONAUTICS

TECHNICAL NOTE NO. 1732

CALCULATED EFFECTS OF GEOMETRIC DIHEDRAL ON THE LOW-SPEED ROLLING DERIVATIVES OF SWEPT WINGS

By M. J. Queijo and Byron M. Jaquet

SUMMARY

A simple theory has been used to determine the effects of geometric dihedral angle on the rolling derivatives of swept wings. Equations and charts are given to show these effects. The analysis indicates that geometric dihedral has an appreciable effect on the lateral force due to rolling, that the damping in roll can be appreciably affected by geometric dihedral under some conditions, and that the yawing moment due to rolling is almost independent of geometric dihedral. The equations have been derived specifically for untapered wings; however, the relations presented are believed to be reasonably reliable for wings of taper ratio as low as 0.5.

Some comparisons are made between calculated and experimental values of the rolling derivatives of an untapered 45° sweptback wing of aspect ratio 2.61 having geometric dihedral angles from -20° to 10°. In general, good agreement between experimental and calculated results was obtained over the low- and moderate-lift-coefficient ranges.

INTRODUCTION

The effects of most of the geometric variables on the aerodynamic characteristics of swept wings at low speeds have been investigated by the application of rigorous or simple theories; however, the effects of geometric dihedral generally have been neglected. The analysis presented in reference 1 for the stability derivatives of swept wings did not include the effects of geometric dihedral, but the methods presented therein can be adapted to include dihedral effects. The method of reference 1 was extended in reference 2 in order to determine the effects of geometric dihedral on the rolling moment due to sideslip and on the rolling moment due to yawing; a similar method of analysis is used herein to determine the effects of geometric dihedral on the stability parameters associated with rolling flight.

Because of the lack of available data for wings with geometric dihedral in rolling flight, a wind-tunnel investigation was made to obtain such data for comparison with results calculated by means of the derived equations. The investigation was conducted in the rolling-flow test section of the Langley stability tunnel on an untapered 45° sweptback wing having an aspect ratio of 2.61, NACA 0012 airfoil sections normal to wing leading edge, and dihedral angles of 10°, 0°, -10°, and -20°. The tests were made at a Mach number of about 0.13 and a Reynolds number of about 1.1×10^6, based on the wing mean aerodynamic chord of 14.16 inches.

SYMBOLS

All forces and moments are given with respect to the system of stability axes shown in figure 1. The origin of the axes is the center of gravity for the airplane in flight. Measured data are given with respect to the quarter chord of the wing mean aerodynamic chord, which is assumed to coincide with the center of gravity. The symbols used herein are defined as follows:

C_L	lift coefficient $\left(\frac{\text{Lift}}{qS}\right)$
c_l	section lift coefficient $\left(\frac{\text{Section lift}}{qc}\right)$
C_Y	lateral-force coefficient $\left(\frac{\text{Lateral force}}{qS}\right)$
C_l	rolling-moment coefficient $\left(\frac{\text{Rolling moment}}{qSb}\right)$
C_n	yawing-moment coefficient $\left(\frac{\text{Yawing moment}}{qSb}\right)$
q	dynamic pressure, pounds per square foot $\left(\frac{1}{2}\rho V^2\right)$
ρ	mass density of air, slugs per cubic foot
V	free-stream velocity, feet per second
S	total wing area (zero dihedral wing), square feet
b	wing span for zero dihedral, feet
c	chord of wing, feet

$\bar{c}$ wing mean aerodynamic chord, feet $\left(\frac{2}{S}\int_0^{b/2} c^2\,dy\right)$

A aspect ratio $\left(b^2/S\right)$

λ taper ratio, ratio of tip chord to root chord

y perpendicular distance from root chord to any point on quarter-chord line (fig. 2), feet

x longitudinal distance rearward from center of gravity to wing quarter chord at any station, feet

$\bar{x}$ longitudinal distance rearward from center of gravity (c.g.) to aerodynamic center (a.c.), feet

z vertical distance between center of gravity and root chord, positive when center of gravity is above root chord, feet

$|\Delta\alpha|$ absolute change in angle of attack caused by rolling velocity, measured in planes parallel to free stream and normal to wing panels, radians

Λ sweep angle, positive for sweepback, degrees

Γ geometric dihedral angle, radians (unless otherwise specified)

$\frac{pb}{2V}$ helix angle generated by wing tip in roll, radians

p angular velocity in roll, radians per second

a_o section lift-curve slope, per radian

$$C_{l_p} = \frac{\partial C_l}{\partial \frac{pb}{2V}}$$

$$C_{Y_p} = \frac{\partial C_Y}{\partial \frac{pb}{2V}}$$

$$C_{n_p} = \frac{\partial C_n}{\partial \frac{pb}{2V}}$$

$\partial C_{l_p}/\partial \Gamma$ rate of change of C_{l_p} with dihedral angle

$\partial C_{Y_p}/\partial \Gamma$ rate of change of C_{Y_p} with dihedral angle

$\partial C_{n_p}/\partial \Gamma$ rate of change of C_{n_p} with dihedral angle

Subscripts:

Γ wings with geometric dihedral

$\Gamma=0^{\circ}$ wings with zero geometric dihedral

$\Lambda=0^{\circ}$ wings with zero sweep

$\Gamma,\Lambda=0^{\circ}$ wings with both zero geometric dihedral and zero sweep

ANALYSIS

Preliminary Considerations

The load on a rolling wing is made up of a symmetrical load caused by the angle-of-attack loading over the entire wing and an antisymmetrical load caused by the rolling velocity. The primary effect of geometric dihedral angle is to tilt the lift vectors about the X-axis through an angle approximately equal to the geometric dihedral angle. Small and moderate geometric dihedral angles would be expected to have little effect on the magnitude or distribution of wing loading; therefore, it would be expected that dihedral effects on aerodynamic induction can be neglected. Because of this assumption, the ratio of an aerodynamic parameter of a wing with dihedral to an aerodynamic parameter of a wing with no dihedral is approximately independent of aerodynamic induction, provided that the two parameters arise from the same flight condition (such as rolling flight, yawing flight, or pitching flight). The ratios of aerodynamic parameters, therefore, may be determined by simple two-dimensional analysis and the ratios would be expected to apply to the three-dimensional case. Although the ratios determined in this manner probably are not very accurate for large dihedral angles (when an appreciable mutual interference occurs between the two wing panels), they are believed to show the proper trends of the derivatives as affected by geometric dihedral.

The absolute change in angle of attack along the semispan of a rolling wing is given by the equation

$$|\Delta\alpha| = \frac{pb}{2V}\left(\frac{y}{b/2} - \frac{z}{b/2}\sin\Gamma\right) \tag{1}$$

The lift-curve slope of a swept-wing panel of infinite span is $a_o \cos\Lambda$; therefore, an increment of lift per unit span is given by

$$\Delta c_l = |\Delta\alpha| a_o \cos\Lambda$$

or, after substitution of equation (1) for $|\Delta\alpha|$, by

$$\Delta c_l = \frac{pb}{2V}\left(\frac{y}{b/2} - \frac{z}{b/2}\sin\Gamma\right)a_o \cos\Lambda \tag{2}$$

Aerodynamic Coefficients

Rolling moment.- According to strip theory, the coefficient of the rolling moment due to rolling for a wing is given by the following equation:

$$\left(C_l\right)_\Gamma = -\frac{2}{qSb}\int_0^{b/2} \Delta c_l (y - z\sin\Gamma) qc\ dy \tag{3}$$

For rectangular wings $c = \frac{S}{b}$; therefore, substituting this value for c in equation (3) and replacing Δc_l with the value given in equation (2) yield

$$\left(C_l\right)_\Gamma = -\frac{1}{2}\int_0^1 a_o \cos\Lambda\ \frac{pb}{2V}\left(\frac{y}{b/2} - \frac{z}{b/2}\sin\Gamma\right)^2 d\left(\frac{y}{b/2}\right)$$

If the equation is integrated and the derivative taken with respect to $\frac{pb}{2V}$, the result is

$$\left(C_{l_p}\right)_\Gamma = -\frac{1}{6} a_o \cos\Lambda\left[1 - 3\frac{z}{b/2}\sin\Gamma + 3\left(\frac{z}{b/2}\right)^2 \sin^2\Gamma\right] \tag{4}$$

For wings with no geometric dihedral, equation (4) becomes

$$\left(C_{l_p}\right)_{\Gamma=0^\circ} = -\frac{1}{6} a_o \cos\Lambda \tag{5}$$

Substituting equation (5) in equation (4) gives

$$\left(C_{l_p}\right)_\Gamma = \left[1 - 3\,\frac{z}{b/2}\sin\Gamma + 3\left(\frac{z}{b/2}\right)^2\sin^2\Gamma\right]\left(C_{l_p}\right)_{\Gamma=0^\circ} \tag{6}$$

The values of $\left(C_{l_p}\right)_{\Gamma=0^\circ}$ to be used in equation (6) should be the values for a wing of the same aspect ratio, taper ratio, and sweep as the wing for which $\left(C_{l_p}\right)_\Gamma$ is being computed. In general, values of $\left(C_{l_p}\right)_{\Gamma=0^\circ}$ are not readily available for swept wings but are available (from experiments or from theory) for unswept wings. According to reference 1,

$$\left(C_{l_p}\right)_{\Gamma=0^\circ} = \frac{(A + 4)\cos\Lambda}{A + 4\cos\Lambda}\left(C_{l_p}\right)_{\Gamma,\Lambda=0^\circ} \tag{7}$$

Therefore, an alternate form of equation (6) is

$$\left(C_{l_p}\right)_\Gamma = \left[1 - 3\,\frac{z}{b/2}\sin\Gamma + 3\left(\frac{z}{b/2}\right)^2\sin^2\Gamma\right]\frac{(A + 4)\cos\Lambda}{A + 4\cos\Lambda}\left(C_{l_p}\right)_{\Gamma,\Lambda=0^\circ} \tag{8}$$

For small dihedral angles $\sin\Gamma \approx \Gamma$ and the term involving $\sin^2\Gamma$ is negligible. With these simplifications, equation (6) reduces to

$$\left(C_{l_p}\right)_\Gamma = \left(1 - 3\,\frac{z}{b/2}\,\Gamma\right)\left(C_{l_p}\right)_{\Gamma=0^\circ} \tag{9}$$

The rate of change of C_{l_p} with geometric dihedral angle can be found by differentiating equation (9) with respect to Γ, and the resulting equation is

$$\frac{\partial C_{l_p}}{\partial\Gamma} = -\,3\,\frac{z}{b/2}\left(C_{l_p}\right)_{\Gamma=0^\circ} \tag{10}$$

Lateral force.- An increment of lateral-force coefficient is introduced by the lateral tilt of the incremental lift vectors and is given by

$$\left(\Delta C_Y\right)_\Gamma = -\frac{2}{qS}\int_0^{b/2} \Delta c_l \sin\Gamma \; qc \; dy \tag{11}$$

or, with the aid of equation (2) and the relation $c = \frac{S}{b}$, by

$$\left(\Delta C_Y\right)_\Gamma = -\int_0^1 a_o \cos\Lambda \frac{pb}{2V}\left(\frac{y}{b/2} - \frac{z}{b/2}\sin\Gamma\right)\sin\Gamma \; d\left(\frac{y}{b/2}\right) \tag{12}$$

If equation (12) is integrated and the derivative is taken with respect to $\frac{pb}{2V}$, the result is

$$\left(\Delta C_{Y_p}\right)_\Gamma = -a_o \cos\Lambda \sin\Gamma\left(\frac{1}{2} - \frac{z}{b/2}\sin\Gamma\right) \tag{13}$$

or, with the use of equation (5),

$$\left(\Delta C_{Y_p}\right)_\Gamma = 3\sin\Gamma\left(1 - 2\frac{z}{b/2}\sin\Gamma\right)\left(C_{l_p}\right)_{\Gamma=0^\circ} \tag{14}$$

Equation (14) expresses an increment of lateral force due to rolling caused by the geometric dihedral angle. This increment must be added to the part of the derivative that results from sweep angle in order to get the total value of C_{Y_p}. The part of C_{Y_p} resulting from sweep angle is given in reference 1 as

$$\left(C_{Y_p}\right)_{\Gamma=0^\circ} = C_L \frac{A + \cos\Lambda}{A + 4\cos\Lambda}\tan\Lambda \tag{15}$$

The total derivative $\left(C_{Y_p}\right)_\Gamma$ therefore is

$$\left(C_{Y_p}\right)_\Gamma = \left(C_{Y_p}\right)_{\Gamma=0^\circ} + \left(\Delta C_{Y_p}\right)_\Gamma \tag{16}$$

With the use of equations (14), (15), and (7), equation (16) can be expressed by

$$\left(C_{Y_p}\right)_\Gamma = C_L \frac{A + \cos \Lambda}{A + 4 \cos \Lambda} \tan \Lambda$$

$$+ 3 \frac{(A + 4) \cos \Lambda}{A + 4 \cos \Lambda}\left(1 - 2 \frac{z}{b/2} \sin \Gamma\right) \sin \Gamma \left(C_{l_p}\right)_{\Gamma, \Lambda=0^\circ} \tag{17}$$

If the value of Γ is assumed to be small, $\sin \Gamma = \Gamma$ and terms involving $\sin^2\Gamma$ are negligible; therefore, equation (14) can be written as

$$\left(\Delta C_{Y_p}\right)_\Gamma = 3\Gamma\left(C_{l_p}\right)_{\Gamma=0^\circ} \tag{18}$$

The rate of change of C_{Y_p} with dihedral angle is found by differentiating equation (18) with respect to Γ; therefore,

$$\frac{\partial C_{Y_p}}{\partial \Gamma} = 3\left(C_{l_p}\right)_{\Gamma=0^\circ} \tag{19}$$

Yawing moment.- Geometric dihedral causes an increment in yawing moment which is associated with the increment in lateral force discussed in the section entitled "Lateral force." This increment in yawing-moment coefficient is given by the following expression:

$$\left(\Delta C_n\right)_\Gamma = \frac{2}{qSb} \int_0^{b/2} \Delta c_l\, qxc \sin \Gamma \, dy \tag{20}$$

or, if the proper substitutions are made with use of equation (2), the relation $c = \frac{S}{b}$, and the relation $x = \left(y - \frac{b}{4}\right)\tan \Lambda + \bar{x}$, by

$$\left(\Delta C_n\right)_\Gamma = \frac{1}{2}\int_0^1 a_o \cos \Lambda \frac{pb}{2V}\left(\frac{y}{b/2} - \frac{z}{b/2} \sin \Gamma\right)\left[\left(\frac{y}{b/2} - \frac{1}{2}\right)\tan \Lambda + \frac{\bar{x}}{b/2}\right]\sin \Gamma \, d\left(\frac{y}{b/2}\right)$$

This equation can be integrated and its derivative taken with respect to $\frac{pb}{2V}$ to give

$$\left(\Delta C_{n_p}\right)_\Gamma = \frac{1}{6} a_o \cos\Lambda\left[\frac{\tan\Lambda}{4} + 3\frac{\bar{x}}{b/2}\left(\frac{1}{2} - \frac{z}{b/2}\sin\Gamma\right)\right]\sin\Gamma$$

or, with the use of equation (5),

$$\left(\Delta C_{n_p}\right)_\Gamma = -\sin\Gamma\left[\frac{\tan\Lambda}{4} + 3\frac{\bar{x}}{b/2}\left(\frac{1}{2} - \frac{z}{b/2}\sin\Gamma\right)\right]\left(C_{l_p}\right)_{\Gamma=0^\circ} \tag{21}$$

Equation (21) is an expression for the increment of C_{n_p} caused by dihedral angle. This increment must be added to the part of C_{n_p} which is independent of dihedral in order to get the total value of the derivative. According to reference 1

$$\left(C_{n_p}\right)_{\Gamma=0^\circ} = C_L\frac{A + 4}{A + 4\cos\Lambda}\left[1 + 6\left(1 + \frac{\cos\Lambda}{A}\right)\left(\frac{\bar{x}}{\bar{c}}\frac{\tan\Lambda}{A} + \frac{\tan^2\Lambda}{12}\right)\right]\left(\frac{C_{n_p}}{C_L}\right)_{\Gamma,\Lambda=0^\circ} \tag{22}$$

The total yawing moment due to rolling is found to be, by substituting equation (7) in equation (21) and adding the values of $\left(\Delta C_{n_p}\right)_\Gamma$ and $\left(C_{n_p}\right)_{\Gamma=0^\circ}$ from equations (21) and (22), respectively,

$$\left(C_{n_p}\right)_\Gamma = C_L\frac{A + 4}{A + 4\cos\Lambda}\left[1 + 6\left(1 + \frac{\cos\Lambda}{A}\right)\left(\frac{\bar{x}}{\bar{c}}\frac{\tan\Lambda}{A} + \frac{\tan^2\Lambda}{12}\right)\right]\left(\frac{C_{n_p}}{C_L}\right)_{\Gamma,\Lambda=0^\circ}$$

$$- \frac{(A + 4)\cos\Lambda}{A + 4\cos\Lambda}\sin\Gamma\left[\frac{\tan\Lambda}{4} + \frac{6}{A}\frac{\bar{x}}{\bar{c}}\left(\frac{1}{2} - \frac{z}{b/2}\sin\Gamma\right)\right]\left(C_{l_p}\right)_{\Gamma,\Lambda=0^\circ} \tag{23}$$

For small dihedral angles $\sin\Gamma \approx \Gamma$, and terms involving $\sin^2\Gamma$ are negligible; therefore, equation (21) reduces to

$$\left(\Delta C_{n_p}\right)_\Gamma = -\Gamma\left(\frac{\tan\Lambda}{4} + \frac{3}{A}\frac{\bar{x}}{\bar{c}}\right)\left(C_{l_p}\right)_{\Gamma=0^\circ} \tag{24}$$

The rate of change of C_{n_p} with Γ is found by differentiating equation (24) with respect to Γ; thus,

$$\frac{\partial C_{n_p}}{\partial \Gamma} = -\left(\frac{\tan \Lambda}{4} + \frac{3}{A}\frac{\bar{x}}{\bar{c}}\right)\left(C_{l_p}\right)_{\Gamma=0^\circ} \tag{25}$$

PRESENTATION OF RESULTS

Calculated values of the parameters $\left(C_{l_p}\right)_{\Gamma,\Lambda=0^\circ}$ and $\left(\frac{C_{n_p}}{C_L}\right)_{\Gamma,\Lambda=0^\circ}$ which can be used in equations (8) and (17), and equation (22), respectively, are presented in figure 3 for aspect ratios from 1 to 16. These charts were obtained from reference 1 and can be used when experimental values of the parameters are not available. Curves of the ratios $\left(C_{l_p}\right)_\Gamma \Big/ \left(C_{l_p}\right)_{\Gamma=0^\circ}$ and $\left(\Delta C_{Y_p}\right)_\Gamma \Big/ \left(C_{l_p}\right)_{\Gamma=0^\circ}$ calculated from equations (6) and (14), respectively, are presented in figure 4 as functions of Γ and $\frac{z}{b/2}$.

Experimental values of the parameters C_{l_p}, C_{Y_p}, and C_{n_p} are plotted in figure 5 as functions of Γ and lift coefficient for an untapered 45° sweptback wing of aspect ratio 2.61. For all configurations $\bar{x}$ was equal to zero, and the distance z was equal to $(b/4)\sin \Gamma$. Experimental values of C_{l_p} are plotted against Γ for several lift coefficients in figure 6. Also shown in figure 6 is the curve of C_{l_p} calculated from equation (8). Cross plots of C_{Y_p} and C_{n_p} are presented in figure 7 as curves plotted against Γ for several lift coefficients. The slopes of the curves of figure 7 were measured and were plotted in figure 8 as curves of $\partial C_{Y_p}/\partial \Gamma$ and $\partial C_{n_p}/\partial \Gamma$ against C_L. Calculated curves of the same parameters are also presented in figure 8. All data were obtained at a test Reynolds number of 1.1×10^6.

The results presented herein have been derived for untapered wings; however, comparisons of results obtained by these equations with results from more complicated equations (based on the same method of analysis) with taper ratio included have indicated that both sets of equations gave approximately the same results for taper ratios as low as 0.5.

DISCUSSION

Calculated Results

Rolling moment.- The analysis presented herein indicates that a combination of large dihedral angle and displacement of the wing root chord from the axis of rotation can produce values of C_{l_p} which are quite different from the values for the same wing with no geometric dihedral (fig. 4). Whether C_{l_p} becomes less negative or more negative with dihedral angle depends on the signs of Γ and $\frac{z}{b/2}$. For small dihedral angles (from about -10° to 10°) C_{l_p} changes linearly with dihedral angle.

Contemporary aircraft generally are designed with small dihedral angles and with the wing root chord close to the center of gravity. This combination of design features tends to make the effect of geometric dihedral angle on C_{l_p} very small.

The contribution of a vee tail to the damping in roll of an airplane changes with angle of attack. If damping in roll is measured about an axis parallel to the flight path and passing through the airplane center of gravity, the distance z is a function of angle of attack and tail length; therefore, for positive dihedral the tail contribution to the airplane C_{l_p} would decrease as the angle of attack increases. This effect should be small unless the tail area is quite large relative to the wing area.

Lateral force.- Geometric dihedral angle has an appreciable effect on lateral force due to rolling as can be seen from figure 4. The effect increases with dihedral angle; for small dihedral angles z has no appreciable effect on the change in C_{Y_p} caused by dihedral, but for larger dihedral angles (greater than $\pm 10^{\circ}$) the distance z affects $\left(\Delta C_{Y_p}\right)_{\Gamma}$ appreciably. Whether $\left(\Delta C_{Y_p}\right)_{\Gamma}$ becomes more positive or more negative with increase in z depends on the signs of z and of Γ.

Yawing moment.- Geometric dihedral causes an increment in yawing moment due to rolling which is almost independent of lift coefficient (equation (21)). The increment is very small and probably would be negligible as a contribution to the values of C_{n_p} of a complete airplane.

Comparison of Experimental and Calculated Results

The data of figure 6 indicate that the method of calculation presented herein can be used to predict values of C_{l_p} quite accurately at low and moderate lift coefficients but that the application of the theory is less reliable at the higher lift coefficients. This difference between calculated and experimental values is primarily due to the fact that the experimental values of C_{l_p} vary with lift coefficient; whereas, theory indicates that C_{l_p} is independent of lift coefficient.

Figure 8 indicates that the theory overestimates the effects of geometric dihedral on C_{n_p} and C_{Y_p} at low lift coefficients and underestimates the effects at high lift coefficients. For the wing used in this investigation, the calculated values of the parameters $\partial C_{Y_p}/\partial\Gamma$ (equation (19)) and $\partial C_{n_p}/\partial\Gamma$ (equation (25)) are approximately equal to the average experimental values of the same parameters.

CONCLUDING REMARKS

An approximate theory has been used to derive equations to indicate the effects of geometric dihedral on the rolling parameters of swept wings. Although the equations presented were derived specifically for untapered wings, the relations presented are believed to be reasonably reliable for wings of taper ratios as low as 0.5.

The theory indicates that lateral force due to rolling shows a marked change with geometric dihedral angle, that yawing moment due to rolling is almost independent of geometric dihedral, and that damping in roll can be changed appreciably if the dihedral angle is large and the displacement of the rolling axis from the wing-root-chord line is moderate or large.

Comparisons between calculated and experimental values of the rolling derivatives for an untapered 45° sweptback wing of aspect ratio 2.61 having geometric dihedral angles from -20° to 10° indicate that the calculated values are fairly reliable over the low- and moderate-lift-coefficient ranges.

Langley Aeronautical Laboratory
National Advisory Committee for Aeronautics
Langley Field, Va., August 24, 1948

REFERENCES

1. Toll, Thomas A., and Queijo, M. J.: Approximate Relations and Charts for Low-Speed Stability Derivatives of Swept Wings. NACA TN No. 1581, 1948.

2. Queijo, M. J., and Jaquet, Byron M.: Investigation of Effects of Geometric Dihedral on Low-Speed Static Stability and Yawing Characteristics of an Untapered 45° Sweptback-Wing Model of Aspect Ratio 2.61. NACA TN No. 1668, 1948.

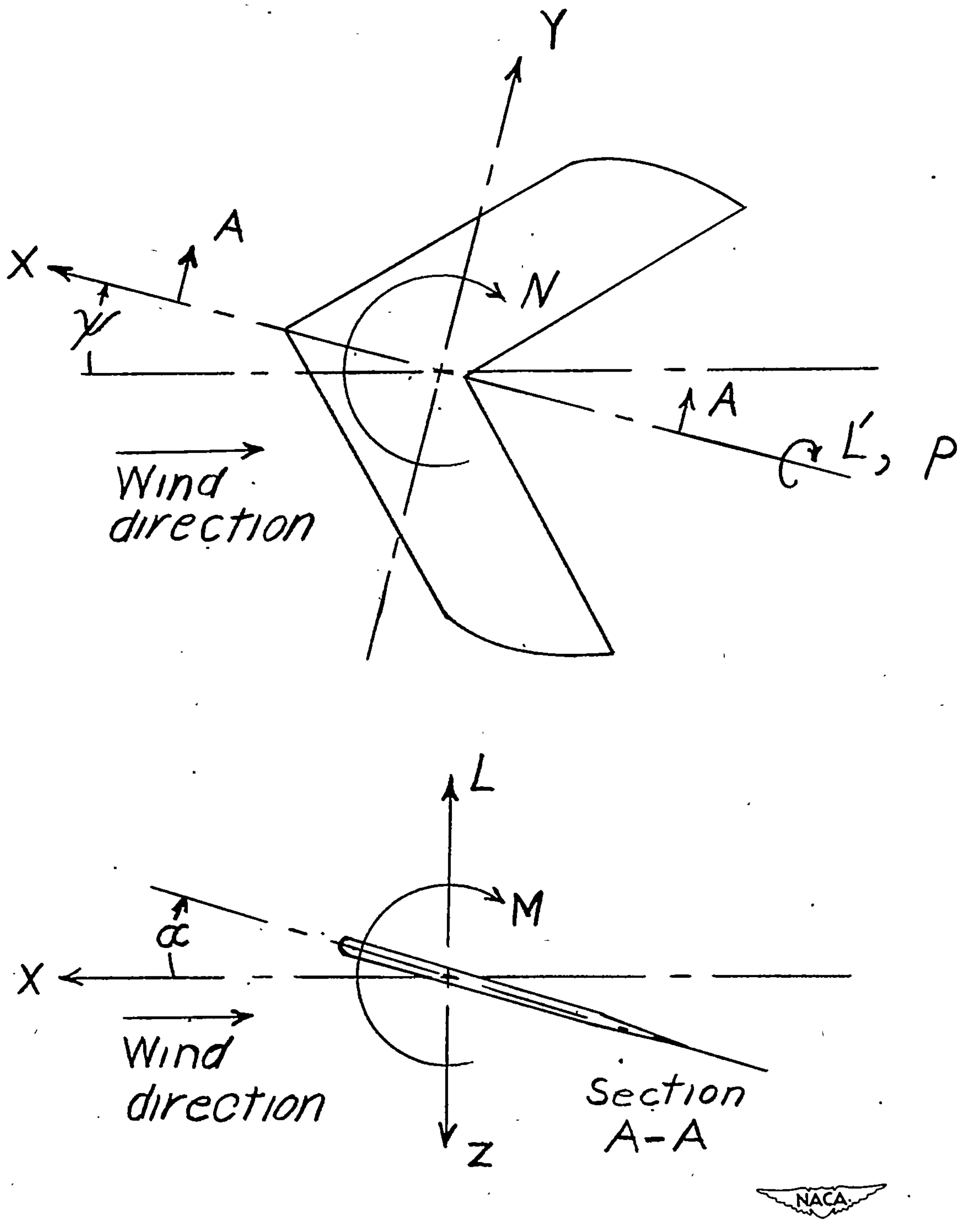

Figure 1.- System of stability axes. Arrows indicate positive directions of forces, moments, and angular displacements.

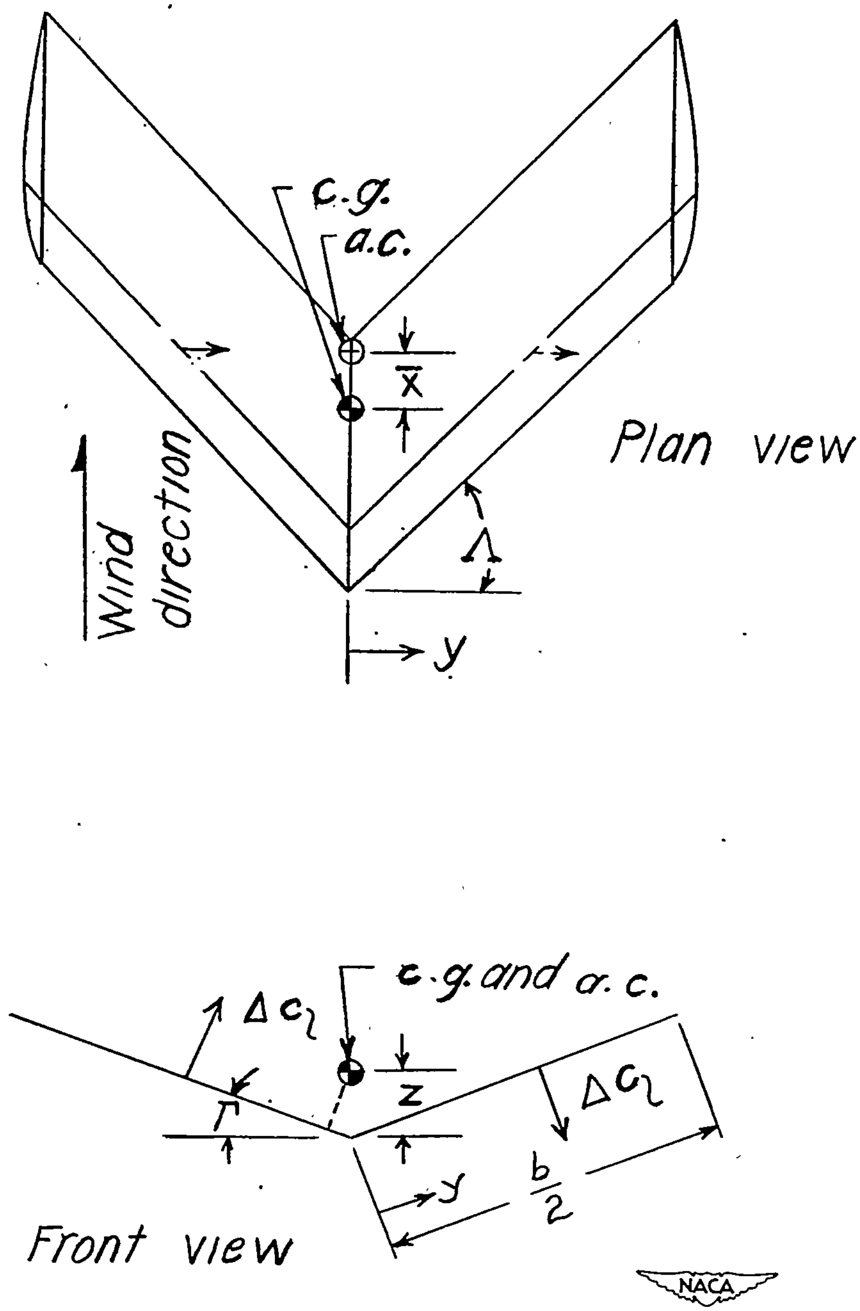

Figure 2.- Force coefficients and geometry considered in the analysis.

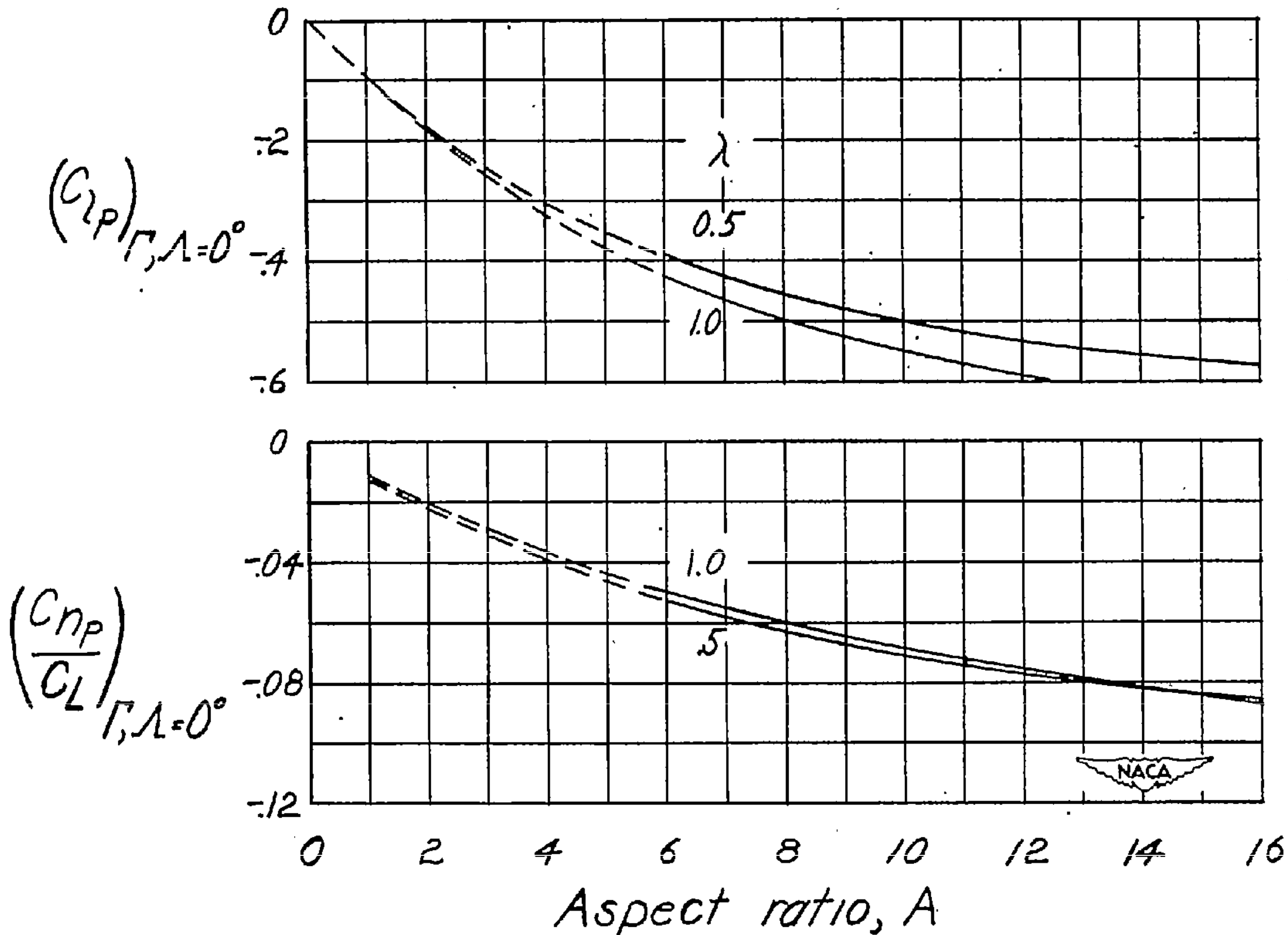

Figure 3.- Calculated values of C_{l_p} and C_{n_p}/C_L for unswept wings with no geometric dihedral. $a_o = 5.67$ (reference 1).

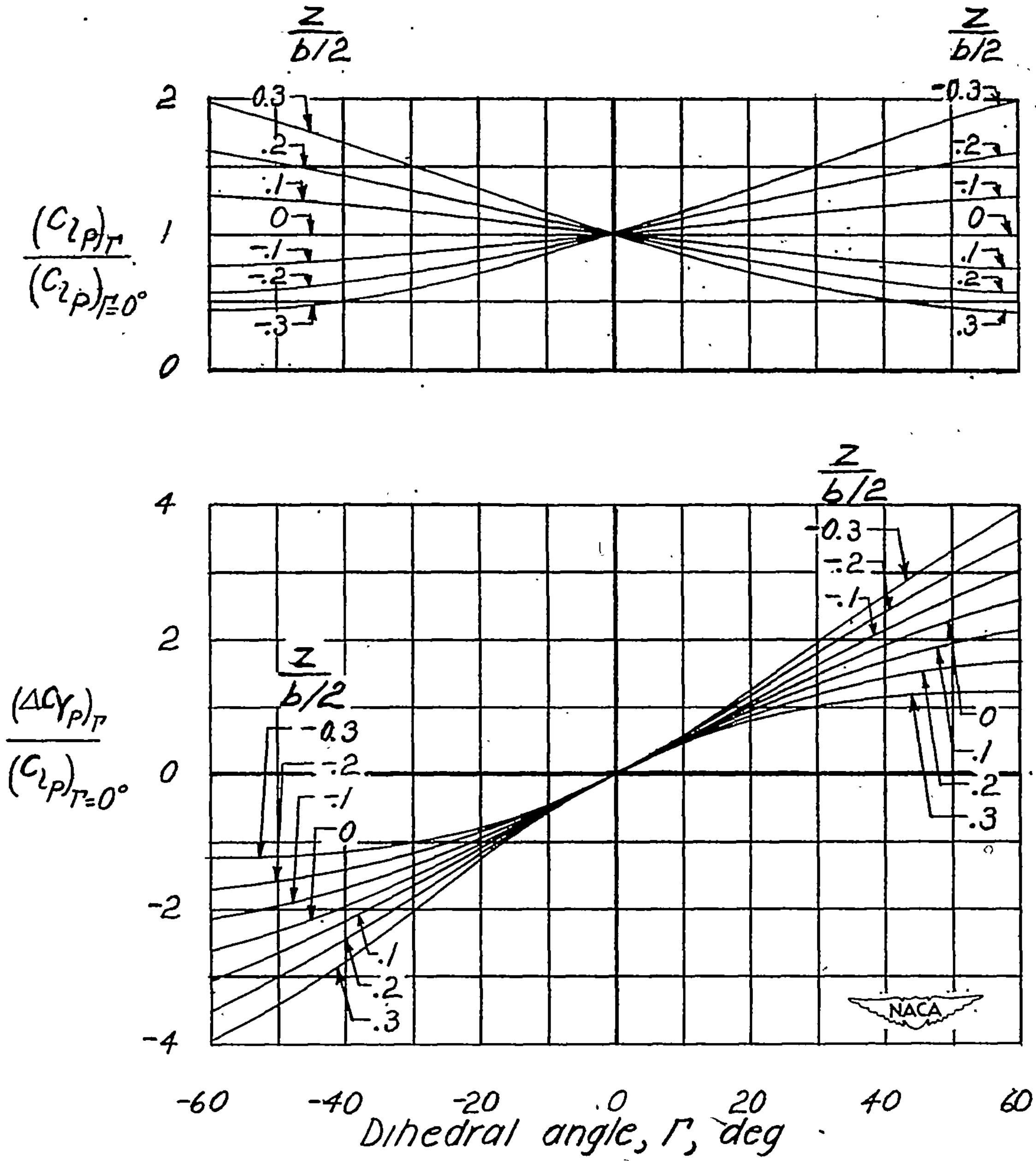

Figure 4.- Chart showing calculated values of the ratios $(C_{l_p})_\Gamma / (C_{l_p})_{\Gamma=0^\circ}$ and $(\Delta C_{Y_p})_\Gamma / (C_{l_p})_{\Gamma=0^\circ}$ (from equations (6) and (14)).

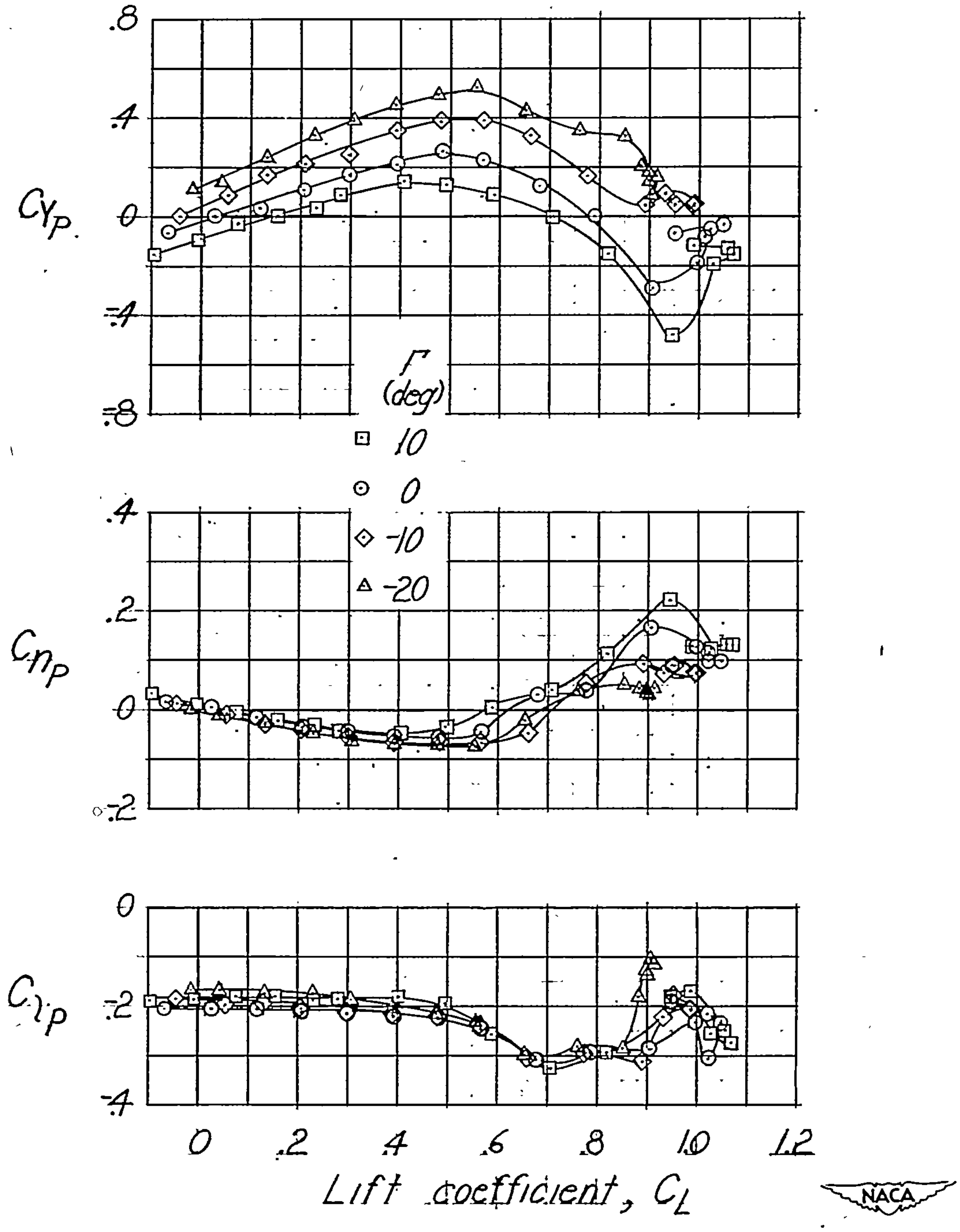

Figure 5.- Experimental values of C_{Y_p}, C_{n_p}, and C_{l_p} for an untapered 45° sweptback wing of aspect ratio 2.61 and various dihedral angles. Reynolds number = 1.1×10^6.

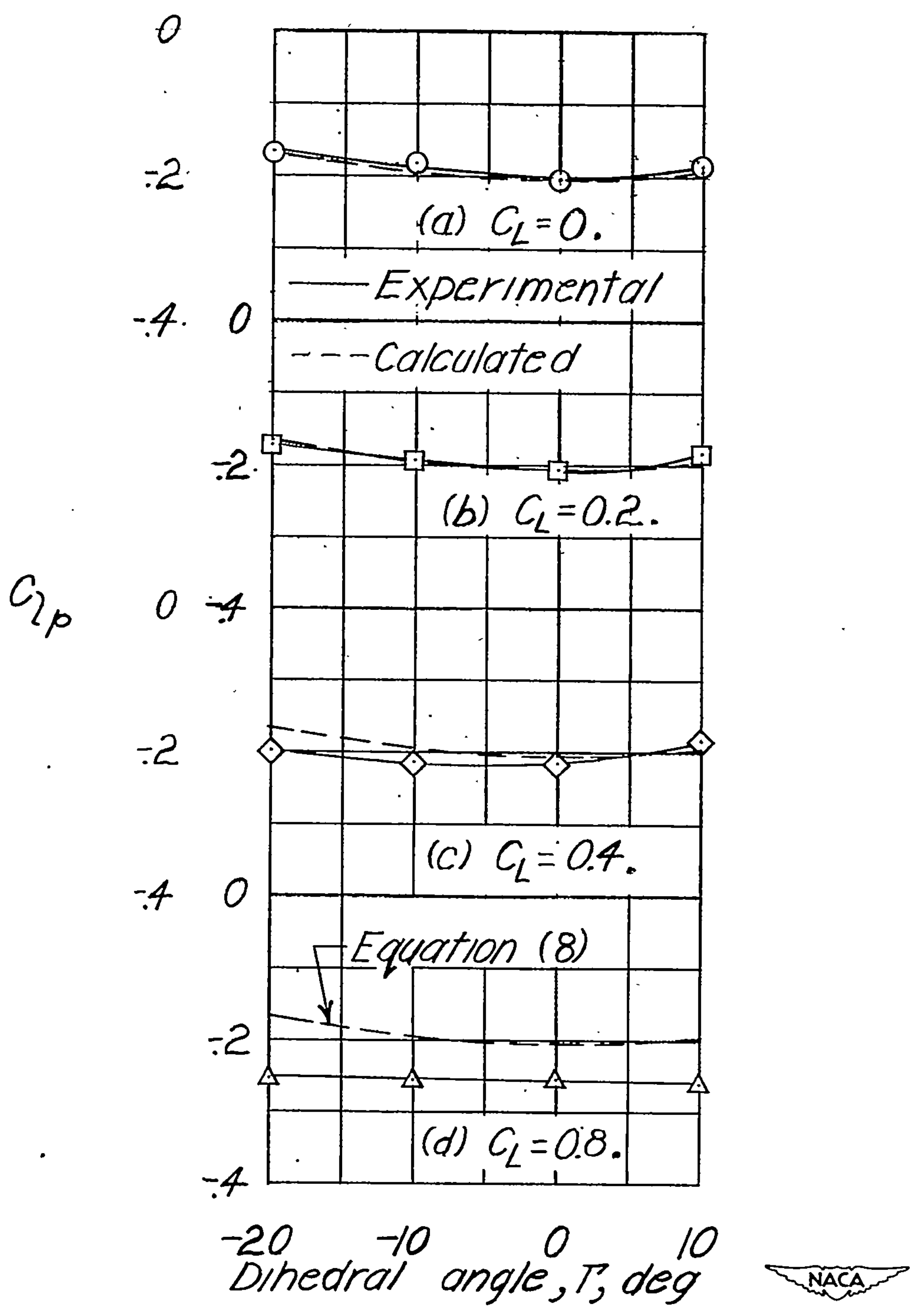

Figure 6.- Comparison of experimental and calculated values of C_{l_p}. $A = 2.61$; $\Lambda = 45^\circ$; test Reynolds number $= 1.1 \times 10^6$.

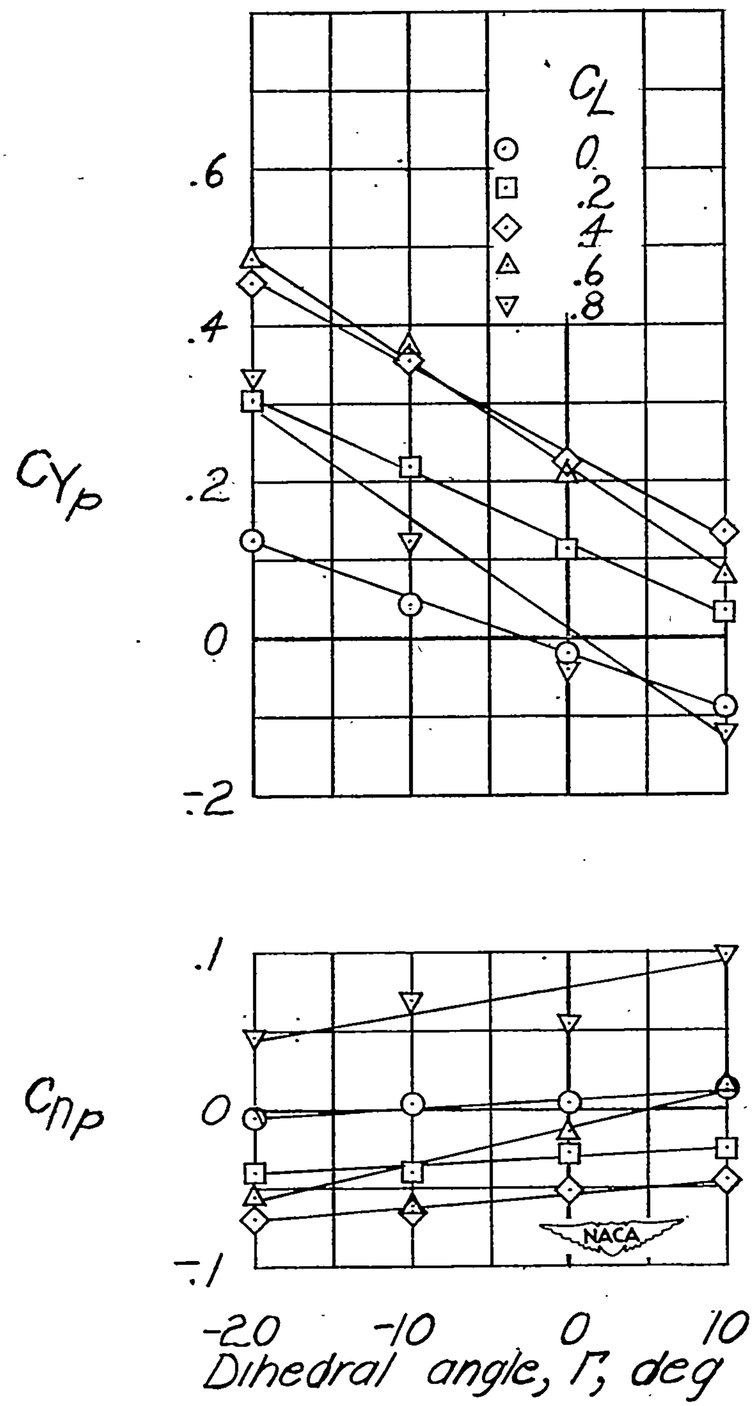

Figure 7.– Experimental variation of C_{Y_p} and C_{n_p} with dihedral angle. $A = 2.61$; $\Lambda = 45^\circ$; test Reynolds number $= 1.1 \times 10^6$.

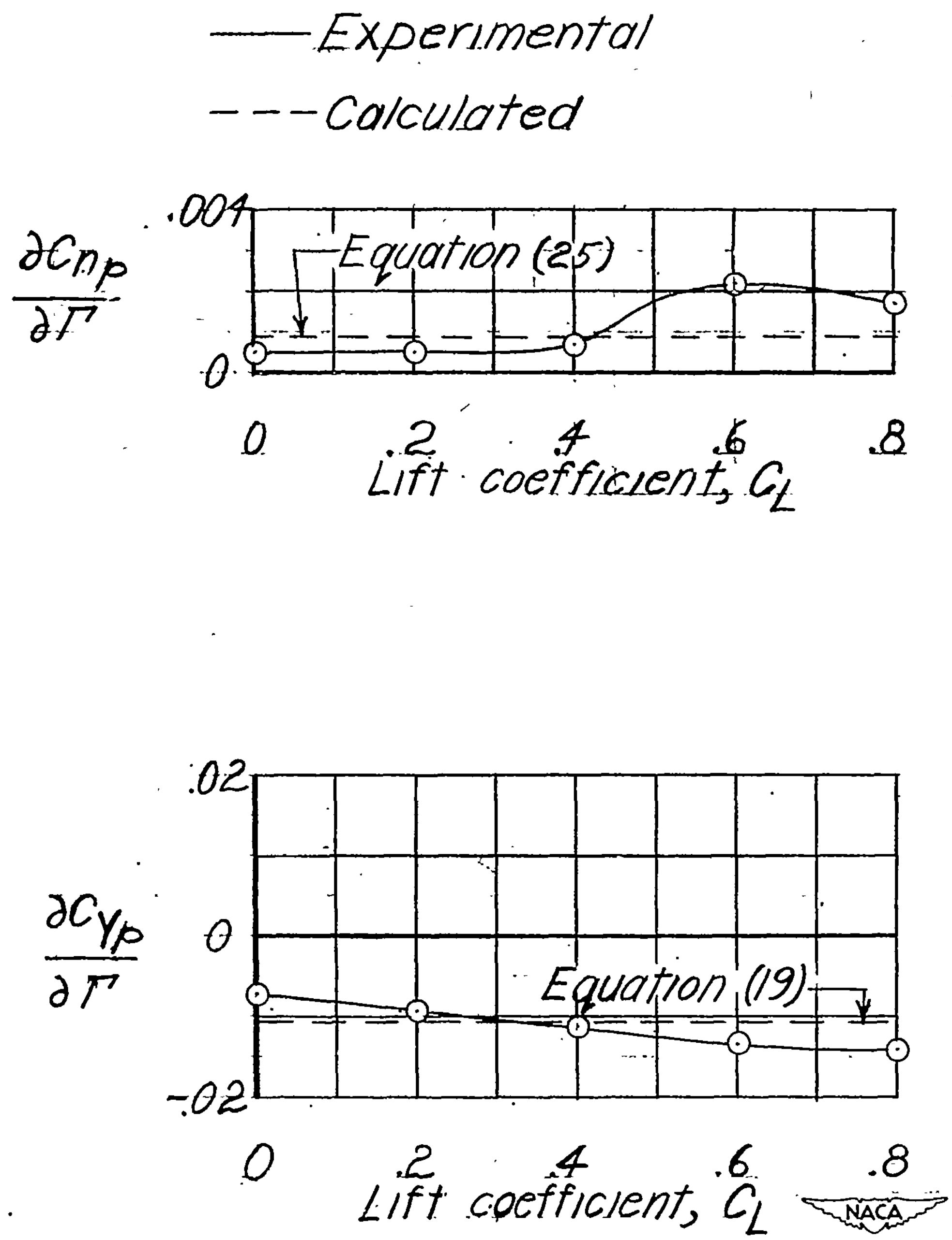

Figure 8.- Comparison of experimental and calculated values of the rate of change of C_{n_p} and C_{Y_p} per degree dihedral.